Cancer Chemother Pharmacol (2010) 66:277–285
DOI 10.1007/s00280-009-1161-z

ORIGINAL ARTICLE

Darbufelone, a novel anti-inflammatory drug, induces growth inhibition of lung cancer cells both in vitro and in vivo

Xiaolei Ye · Wu Zhou · Yongqi Li · Yihua Sun · Yihua Zhang · Hui Ji · Yisheng Lai

Received: 23 June 2009 / Accepted: 6 October 2009 / Published online: 30 March 2010

Abstract
Purpose Inflammation plays a crucial role in the development of lung cancer. Accumulated studies have proved that non-steroidal anti-inflammatory drugs (NSAIDs) which block inflammation by their actions on arachidonic acid (AA) metabolism have a potential role in cancer chemotherapy and chemoprevention. The aim of our study was to investigate whether darbufelone, a novel anti-inflammatory drug, has anticancer effects in lung cancer.
Methods Human non-small cell lung cancer cell lines were treated with darbufelone at various doses and time points for analysis of cell viability, cell cycle, and apoptosis in vitro. The in vivo effect of darbufelone was assessed in Lewis lung carcinoma mice model.
Results Darbufelone inhibited the proliferation of non-small cell lung cancer cell lines in a dose-dependent manner, and induced cell cycle arrest at G0/G1 phase through up-regulation of p27 expression. Treatment with darbufelone also induced apoptosis by activating caspase-3 and caspase-8. Lewis lung carcinoma growth was also significantly inhibited by darbufelone treatment at daily dose of 80 mg/kg.
Conclusions Taken together, these studies suggested that darbufelone, an anti-inflammation drug, might represent a novel therapeutic approach for lung cancer treatment.

Keywords Darbufelone · Anti-inflammatory drug · Arachidonic acid · Lung cancer

Abbreviations

AA	Arachidonic acid
COX-2	Cyclooxygenase-2
5-LOX	5-Lipoxygenase
Darbufelone	Darbufelone mesilate
SCLC	Small cell lung cancer
NSCLC	Non-small cell lung cancer
RT	Reverse transcriptase

Introduction

Lung cancer is the leading cause of cancer-related death in both men and women world-wide, with 1.2 million new cases diagnosed and about one million deaths recorded annually [1]. Non-small-cell lung cancer (NSCLC), including squamous carcinoma, adenocarcinoma, and large cell carcinoma, accounts for more than 80% of all lung cancers [2]. More than half of these patients have lost the opportunities for surgery when diagnosed, and chemotherapy still remains one of the most common therapies. However, existing chemotherapy has reached a plateau of effectiveness in

X. Ye and W. Zhou contributed equally to this work.

X. Ye · Y. Li · H. Ji (✉)
Department of Pharmacology,
China Pharmaceutical University, 24 Tong Jia Xiang,
210009 Nanjing, People's Republic of China
e-mail: huijicpu@163.com

Y. Zhang · Y. Lai (✉)
Center of Drug Discovery, China Pharmaceutical University,
24 Tong Jia Xiang, 210009 Nanjing, People's Republic of China
e-mail: yishenglaicpu@163.com

W. Zhou
Institute of Immunology, Zhejiang University,
210058 Hangzhou, People's Republic of China

Y. Sun
Department of Thoracic Surgery,
Shanghai Cancer Hospital, Fudan University,
20032 Shanghai, People's Republic of China

improving the survival of NSCLC patients. It is urgent to explore new therapies that are designed to interfere with some other aberrant biologic signal pathways.

Arachidonic acid (AA) pathway plays an important role in inflammation. In early 1980s, it was reported that aberrant AA metabolism participated in the carcinogenic processes [3]. AA metabolites derived from either cyclooxygenase (COX) or lipoxygenase (LOX) reaction transduce a variety of signals related to cell proliferation, differentiation, and inflammation [4]. COX-2 and 5-LOX, as isoforms of COX and LOX, respectively, are two key enzymes in the downstream of the AA pathway. A series of studies have shown that COX-2 is up-regulated in patients with lung cancers associated with poor prognosis [5–7]. COX-2 inhibition by celecoxib has been proved to inhibit the growth of lung-cancer cells in vitro and in vivo [8]. 5-LOX inhibition has also been demonstrated to prevent lung tumorigenesis in carcinogen-treated mice [9]. These data suggest that inhibition of either enzyme can benefit lung cancer treatment. Hence we hypothesized that the dual inhibitor of COX-2 and 5-LOX might be more potent in lung cancer treatment. Darbufelone (also known as CI-1004, Fig. 1a) [10], as a novel anti-inflammatory drug which blocks the activity of both COX-2 and 5-LOX, is currently being evaluated in Phase III clinical trials for the treatment of rheumatoid arthritis [11]. Yet there are no available data evaluating its anticancer effect. We seek to test the hypothesis that darbufelone has a potent anti-cancer effect on non-small-cell-lung cancer cells.

Our results demonstrate for the first time that darbufelone is able to induce cell cycle arrest and trigger apoptosis in human lung cancer cells in vitro and impair the Lewis lung cancer growth in vivo. These results suggest that darbufelone may represent a novel therapeutic approach for lung cancer treatment.

Materials and methods

Reagents

Darbufelone mesilate was kindly provided by Center of Drug Discovery, China pharmaceutical university, MTT (3-(4,5-dimethylthiazol-2-yl)-2,5-diphenyltetrazolium bromide) was purchased from Sigma Chemical Co. Annexin V–FITC/PI apoptosis detection kit was purchased from KeyGEN Biotech Co (Cat No: KGA106, Nanjing, China). Primary antibody anti-β-actin (1:1,000) was from Sigma Chemical Co (Cat No: A2228); anti-p27 (sc-528,1:1,000), anti-Bcl-2 (sc-7382,1:300), anti-Bax (sc-493,1:300), anti-caspase-3 (sc-7148,1:1,000), and anti-caspase-9 (sc-8355, 1:200) were from Santa Cruz Biotechnology (Santa Cruz, CA, USA); anti-caspase-8 (559932,1:1,000) was from BD bioscience. Monoclonal and polyclonal horse radish peroxidase-conjugated secondary antibodies (1:1,000) were from Sigma Chemical Co.

The primers were synthesized by the Shanghai Sangon Biological Engineering Technology & Services Co., Ltd.

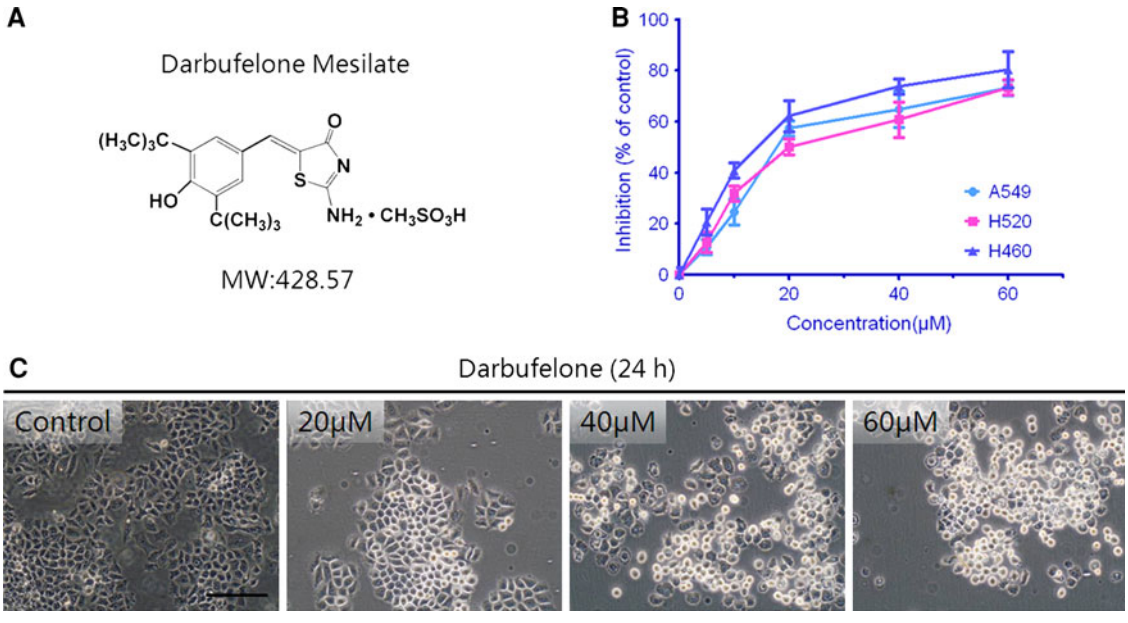

Fig. 1 Darbufelone decreases H460 cell viability in a dose-dependent manner. **a** Chemical structure of darbufelone mesilate. **b** Viability inhibition of A549, H520, and H460 cell lines was determined by MTT assay after treatment with darbufelone (5–60 μM) for 72 h. Results are expressed as percentage mean ± SEM of three independent experiments. **c** Different morphology changes of H460 cells were photographed after treatment with darbufelone (20, 40, 60 μM, respectively) for 24 h (*bar scale* 100 μm)

RNA extract reagent TRIzol and reverse-transcriptase PCR (RT-PCR) kits were bought from Invitrogen.

Cell cultures and treatments

A549 (CCL-185, lung adenocarcinoma cancer cell line), NCI-H520 (HTB-182, lung squamous cancer cell line) and NCI-H460 (HTB-177, lung large cell cancer cell line) cells were purchased from ATCC. All cell lines were cultured in RPMI-1640 (Hyclone, Beijing, China), supplemented with 10% (v/v) heat-inactivated fetal bovine serum (Gibco), 2 mM L-glutamine, 100 U/ml penicillin G, and 100 μg/ml streptomycin (Sigma). Cells were grown at 37°C in a humidified atmosphere of 95% air and 5% CO_2 and routinely passaged using 0.25% trypsin–EDTA (Gibco).

Darbufelone was dissolved in DMSO (dimethyl sulfoxide, Sigma) and diluted into the medium to obtain the required final concentration before each experiment. Control samples were treated in parallel with an equivalent concentration of DMSO.

Cell growth inhibition assay

The effect of darbufelone on human lung carcinoma cell viability was determined by MTT reduction assay. In brief, tumor cells growing in log-phase were trypsinized and seeded at 5×10^3 cells per well into 96-well plates and allowed to attach overnight. Medium in each well was replaced with fresh medium or medium containing various concentrations of drugs in at least triplicate wells. Cells were cultured to another 72 h. After treatment, 1/10 volume of MTT solution (5 mg/ml) was added to each well, and the plate was incubated at 37°C for another 4 h. Two hundred microliters of DMSO was added to each well to solubilize the MTT-formazan product after removal of the medium. Absorbance at 595 nm was measured with a multi-well spectrophotometer (Thermo, USA). Growth inhibition was calculated as a percentage of the untreated controls.

Nuclear morphological changes

Morphological changes in the nuclear chromatin of cells undergoing apoptosis were detected by the DNA-binding DAPI staining (DAPI, Sigma). Briefly, H460 cells were seeded on a six-well plate at the density of 6×10^5 cells/ml and cultured in the presence or absence of darbufelone for the indicated times. At the end of incubation, 1 μg/ml DAPI was added to each well for 5 min at 37°C in the dark. Cells were then washed with PBS (phosphate buffered saline) and promptly observed under a fluorescence microscope (Nikon Eclipse 90i, Nikon Instruments, Japan).

Flow cytometry analysis

For the analysis of DNA content, H460 cells were seeded on a six-well plate at the density of 6×10^5 cells/ml and then cells were starved for 24 h for culture synchronization. After that, cells were incubated with darbufelone for 24 and 48 h, respectively. At the end of incubation, cells were harvested by trypsinization, washed in PBS, and incubated at 4°C for 1 h in the DNA-staining solution containing 50 μg/ml propidium iodide (PI) and 20 μg/ml RNase A. DNA content analysis was performed by FACS Calibur (Becton Dickinson). Cell cycle analysis was executed by Dean-Jett-Fox model.

Annexin V–FITC and propidium iodide double staining assay

Phosphatidylserine (PS) translocation from the inner to the outer leaflet of the plasma membrane in H460 cells was detected with an annexin V–FITC/PI apoptosis detection kit (KeyGEN, Nanjing, China). After being exposed to darbufelone for indicated time points, 5×10^5–5×10^6 cells/ml cells were harvested with 0.25 % trypsin and washed twice with PBS for 5 min at 2,000 g. The supernatant was discarded and the pellet was resuspended in 500 μl 1× binding buffer. 5 μl of annexin V–FITC solution and 5 μl of dissolved PI were added to the cell suspensions. The samples were mixed gently and incubated at room temperate for 5–15 min in the dark. Then the cell preparations were analyzed by FACS Calibur (Becton Dickinson).

Reverse-transcriptase PCR

Cells were seeded on 6 cm dishes and treated with darbufelone at 20 μM and harvested at different time points with trypsin, then washed twice with PBS, and collected by centrifugation at 1,000*g* for 5 min. Total RNA was extracted using Trizol reagent (Invitrogen) following the manufacture's protocol. cDNA was generated with Oligo-dT primers. Primers were designed online using the primer 3 designer program (website: http://frodo.wi.mit.edu/) and were as follows:

p21: forward, 5′-AGA CAC CAC TGG AGG GTG AC-3′; reverse, 5′-GGA TTA GGG CTT CCT CTT GG-3′. p27: forward, 5′-AGA TGT CAA ACG TGC GAG TG-3′; reverse, 5′-TGC GTG TCC TCA GAG TTA GC-3′. p53: forward, 5′-CCT CAC CAT CAT CAC ACT GG-3′; reverse, 5′-CCT CAT TCA GCT CTC GGA AC-3′. GAPDH (housekeeping gene): forward, 5′-GGA GAT TGT TGC CAT CAA CG-3′; reverse 5′-TTG GTG GTG CAG GAT GCA TT-3′. The reaction systems were 0.2 μl of cDNA, 2.5 μl of 10× Taq enzyme buffer, 1 μl of 10 mol/l dNTP, 0.2 μl of each primers and 0.2 μl of Taq enzymes,

then water was added to 25 μl. PCR conditions were as follows: denature at 95°C for 2 min; each cycle consisting of 1 min at 94°C, 1 min 56°C; 1 min and 15 s at 72°C; and a final extension of 5 min at 75°C. After the reaction, the PCR products were separated in 2% agarose gel and visualized under UV light.

Western blotting

Western blotting was performed for whole cell lysate. Briefly, exponentially growing cells were exposed to darbufelone and then collected at different time points, and protein was extracted as previously described [12]. Aliquots of total protein (50 μg per lane) were electrophoresed on 10% SDS-polyacrylamide gels and transferred to nitrocellulose membranes (Amersham). Non-specific binding was blocked by incubation in TBS-T (50 mM Tris, pH 8.0, 150 mM NaCl, 0.1% Tween-20) with 5% dried milk for 1 h at room temperature. Membranes were incubated for 2 h at room temperature with various antibodies. After washing with TBS-T, the membranes were incubated with horseradish peroxidase-conjugated immunoglobulin secondary antibody (sigma) 1:5,000 diluted in TBS-T for 1 h at room temperature, followed by development with enhanced chemiluminescence reagents (Amersham) and exposure to X-ray film. Bands were analyzed by Tanon GIS software 4.0 (Tanon, China) and were normalized to actin levels.

Treatment of Lewis lung carcinoma

C57Bl/6 male mice at 4–5 weeks were obtained from Qinglong Mountain Farm (Nanjing, China). These mice were housed in air-conditioned quarters and were provided food and water ad libitum. All animals were treated according to the guidelines of the Animal Care and Use Committee of China Pharmaceutical University.

The Lewis lung carcinoma (LLC) was kindly provided by Professor Qinglong Guo (China Pharmaceutical University, PR China). On the day 0, Lewis Lung Carcinoma cells (1×10^6) were implanted into the left armpit of C57Bl/6 mice. The mice were randomly divided into four treatment groups of ten animals each. The day after inoculation (day 1), control group was treated with CMC-Na, and other groups were administered Darbufelone by gavage at doses of 20, 40, and 80 mg/kg/day. The treatment was continued till the end of the study. On day 14, animals were killed, and tumors were excised, weighed, and fixed in formalin for the further histochemical analysis.

Immunohistochemistry

For immuno-histochemical staining, tumor tissues were paraffin-embedded and sectioned at 5 μm. The sections were heat-immobilized, deparaffinized by xylene, rehydrated in a graded series of ethanol and washed with distilled water. For antigen unmasking, the tumor sections were boiled in 10 mM sodium citrate buffer (pH 6.0) for 7 min and cooled to room temperature (RT). After washing with TBS-T (Tris buffered saline containing 0.1% Tween-20), endogenous peroxidase activity was blocked by incubation in 3% H_2O_2 in methanol for 10 min at RT. Then the sections were stained with antibodies for Ki-67 (ZA-0502, ZhongShan Goldbridge, Beijing, PR China) which was 1:100 diluted in antibody dilution buffer, or for cleaved caspase-3 (#9661, Cell Signaling Technology, Co. LTD) which was 1:150 diluted in antibody diluted buffer, using ABC and DAB kits according to the manufacturers' protocols and counterstained with Mayer's hematoxylin solution. Six high-power fields (×400) were photographed and scored per section under an Eclipse 80i (Nikon, Japan) microscope. Either positively stained or unstained cells were quantified in six random fields (irrespective of staining intensity). One thousand cells were calculated and the results were expressed as an average percentage of positive cells for either Ki-67 or cleaved caspase-3.

Statistics

All data were expressed as mean ± SEM. Statistical analysis was performed using the student's t test or one-way ANOVA followed by the post hoc Tukey's test. A value of $p < 0.05$ was considered to be statistically significant.

Results

Darbufelone treatment reduced the viability of NSCLC cell lines

To test the putative anti-proliferative effect of the anti-inflammatory drug, darbufelone, we chose A549, H520 and H460 cell lines,which were established from three distinct pathological subtypes of NSCLC (adenocarcinoma, squamous and large cell lung cancer respectively). Since this was the first study to assess the effect of darbufelone on human lung cancer cell viability, increasing concentrations of this drug, ranging from 5 to 60 μM, were tested for 72 h. As shown in Fig. 1b, the cell growth inhibition of these three cell lines gradually increased with higher drug concentration. The IC50 (half maximal inhibitory concentration) of A549 and H520 were 20 ± 3.6 and 21 ± 1.8 μM, respectively, while the H460 has much lower IC50 (15 ± 2.7 μM) (Fig. 1b). Therefore, H460 was chosen for further studies. It is noteworthy that darbufelone, after 24 h of incubation, dramatically affected H460 cell morphology, as the treated cells turned round, detached from the culture

dishes, and membrane bleb formed (Fig. 1c), suggesting the occurrence of apoptosis.

Darbufelone treatment induced G1 growth arrest potentially through p27 up-regulation

The effect of darbufelone on cell cycle progression of H460 was analyzed by flow-cytometry. After 24 h of drug treatment, the percentage of H460 cells in G0/G1 phase increased, while cells in G2/M phase decreased, and the proportion of S-phase cells was not affected (Fig. 2a, b). After incubation with darbufelone for 48 h, a substantial hypodiploid (Sub G1) peak, which represented apoptotic cells, appeared at the concentration of 40 and 60 μM (Fig. 2).

With findings above, we decided to use the low-concentration darbufelone (20 μM) to analyse darbufelone's effect on cell cycle associated proteins. H460 cells harboring wild-type p53 gene had abundant p53 mRNA (Fig. 2c) [13]. The mRNA level of p53 and p21 showed no change after exposure to darbufelone for different time. In contrast, the mRNA level of p27 increased in a time-dependent manner. Consistently, western blotting of p27 (Fig. 2d) also showed an increase of p27 protein level, suggesting that cell cycle arrest induced by darbufelone might be related to the increased p27 protein level.

Darbufelone treatment triggered apoptosis

As shown in Fig. 2, incubation of higher dose of darbufelone for 24 h did not result in increased G0/G1 phase proportion. Alternatively, an increased Sub G1 phase emerged, which was evident in cells treated with darbufelone (60 μM) for 48 h, suggesting the occurrence of apoptosis at higher concentration. We performed DAPI staining to confirm the appearance of apoptosis (Fig. 3a). Although low concentration of darbufelone (20 μM) did not induce significant cell apoptosis, the typical apoptotic feature, such as irregularly fragmented pycnotic nuclei, was evident after 48-h treatment of darbufelone (60 μM) which was accompanied by a dramatic decrease of cell number as well. These observations were further confirmed by annexin V/PI double staining. As shown in Fig. 3b, exposure to darbufelone for 48 h increased H460 cell deaths in time-dependent manner. The proportion of AV^+/PI^+ (later apoptosis), after 36 h-darbufelone treatment increased from 11.23 to 43.22%, while the proportion of AV^-/PI^- (viable cells) decreased from 85.57 to 12%. Likewise, in the 48-h darbufelone treatment group, the proportion of late apoptotic cells increased to 32.23%, and that of AV^-/PI^- (viable cells) decreased to 1.31%. These data suggested that darbufelone induced H460 cell apoptosis through a time-dependent way at the dose of 60 μM.

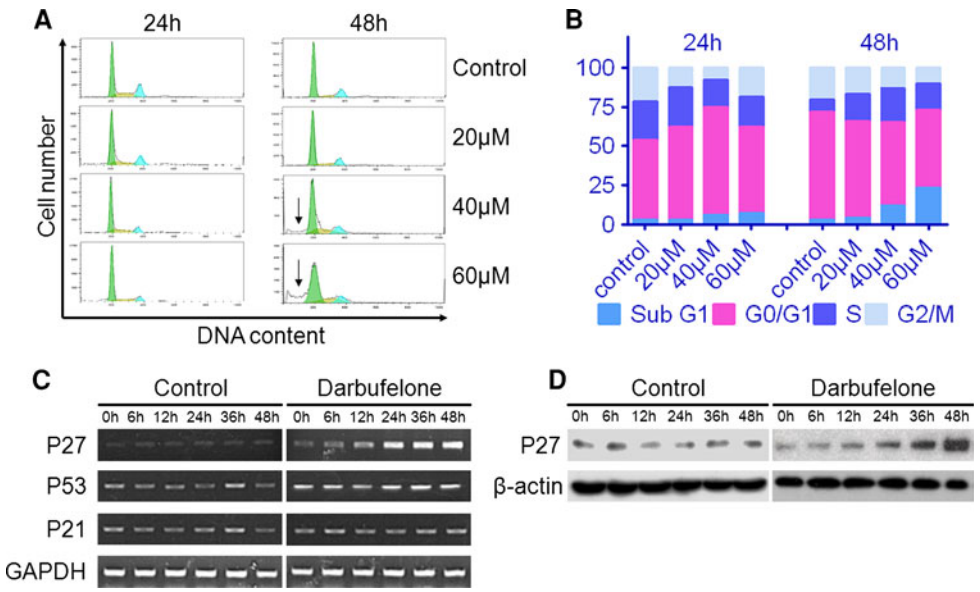

Fig. 2 Darbufelone affects cell cycle of H460 cells. **a** Flow cytometry analysis of PI stained H460 cells revealed significant sub-G1 peaks after treatment with 40 and 60 μM darbufelone for 48 h compared with controls (indicated by *arrows*). **b** Cell cycle distribution in **a** was quantified and histograms showed different cell cycle proportions consistent with different incubating time and concentrations of darbufelone. An increase was observed in G0/G1 phase at 24 h and in Sub-G1 phase at 48 h. **c** Darbufelone increased the mRNA level of p27 in a time-dependent manner. H460 cells were harvested at different time points after treatment with or without darbufelone, and mRNA levels of p53, p27, p21, and GAPDH (internal control) were detected by PT-PCR. **d** The protein level of p27 in H460 cells treated with or without 20 μM of darbufelone was evaluated by western blot. Darbufelone increased the expression of p27 in a time-dependent manner compared with control group

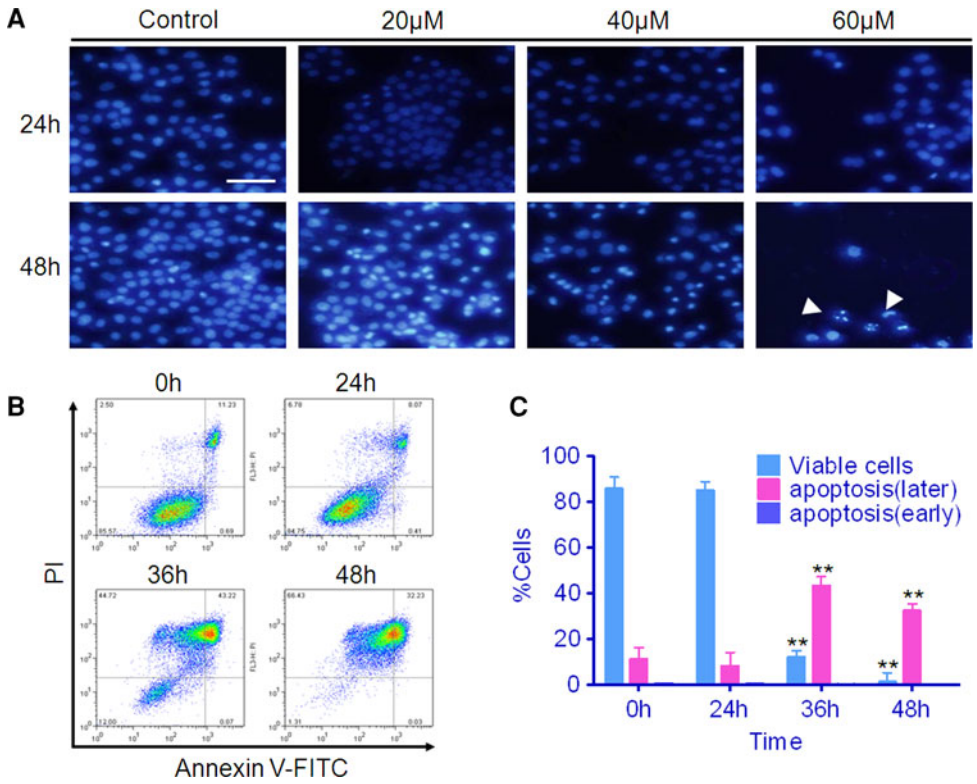

Fig. 3 Darbufelone induces apoptosis in H460 cells. **a** Fluorescence microscopy analysis of H460 cells incubated with darbufelone 20–60 μM for 24 and 48 h and stained with DAPI (*bar scale* 100 μm). A typical apoptotic figure, such as irregularly fragmented pycnotic nuclei, was observed in treated cells at 48 h. **b** H460 cells were exposed to 60 μM of darbufelone for 0, 24, 36, and 48 h, respectively. Cells were harvested and apoptotic cells were detected by flow cytometry with annexin V/PI double staining. The lower left quadrants represent the viable cells, the lower right quadrant the early apoptotic cells (represent early stage of apoptosis), and the upper right quadrant the late apoptotic cells (represent late stage of apoptosis). **c** The proportions of early and late apoptotic H460 cells by flow cytometry assay as in **b** were quantified. Histograms showed the percentages of viable cells, early and late apoptotic H460 cells exposed to different time course with darbufelone. The data expressed as the percentages of cells were the mean ± SEM of three separate experiments (*$p < 0.05$ vs. control, **$p < 0.01$ vs. control)

Darbufelone treatment induced apoptosis through activation of caspase-3 and caspase-8

Activation of caspase-3 is crucial to the process of apoptosis. We found that 60 μM of darbufelone induced, starting from 24-h treatment onward, a strong and time-dependent cleavage of the 34-kDa pro-enzyme caspase-3 into its active 17 kDa form (Fig. 4a, b).

Caspase-3-involved apoptosis can be mediated either through activation of the tumor necrosis receptor family members via caspase-8 cleavage (extrinsic pathway) or through the mitochondria that involves activation of caspase-9 (intrinsic pathway). We sought to determine which pathway of apoptosis was activated by darbufelone. H460 cells were incubated with or without darbufelone (60 μM) for 48 h, and processing of caspase-8 and caspase-9 were investigated. Our data showed that pro caspase-8 was cleaved with time after darbufelone treatment (Fig. 4c). In contrast, we could not detect any significant change in caspase-9 expression (Fig. 4d). No changes in the level of the Bcl-2 and Bax (Fig. 4e), and the ratio of Bcl-2/Bax remained almost same (data not shown). These data suggested that darbufelone promotes programmed cell death of H460 cells through the activation of caspase-3 and caspase-8 which may be involved in extrinsic pathway of apoptosis.

Darbufelone treatment inhibited tumor growth in Lewis lung cancer mice model

In order to demonstrate the anti-tumor effect of darbufelone in vivo, we employed the Lewis lung cancer mice model. Tumor growth was monitored every other day for 14 days. There was no significant difference of body weight between vehicle control group and darbufelone-treated group. Side effects such as lethargy and mortality were not observed in mice with darbufelone treatment. When mice were treated with darbufelone at dosage of 80 mg/kg/day, we observed that the tumor volumes decreased in a time-dependent manner (Fig. 5a). In contrast, lower dose of darbufelone (20 or 40 mg/kg/day) did not show any significant inhibition of

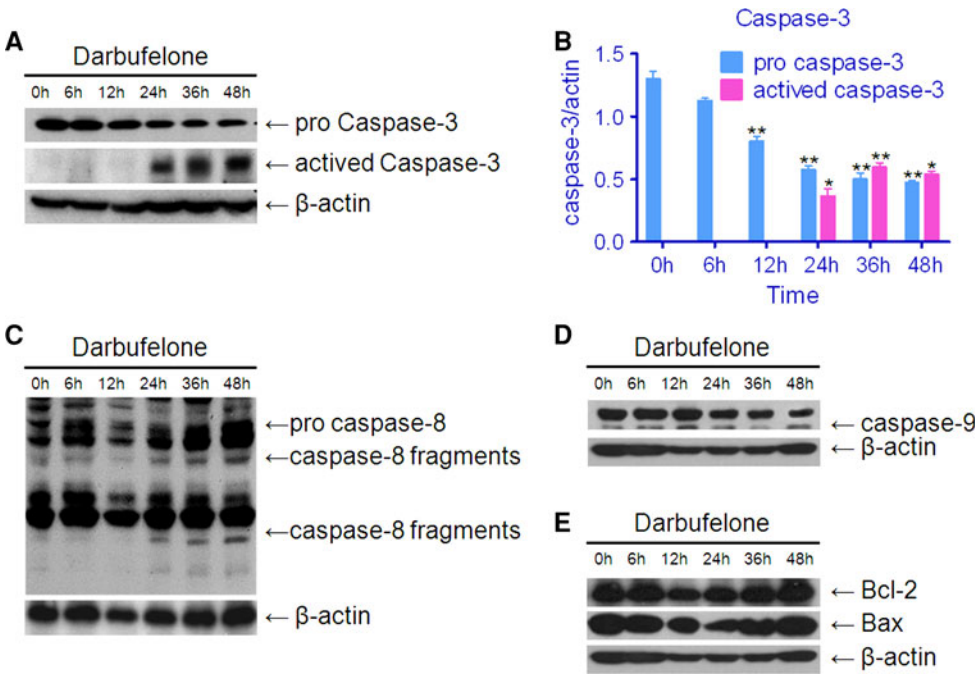

Fig. 4 Darbufelone induces apoptosis in H460 cells through caspase-3 and caspase-8 activation. **a** Time course of caspase-3 activation, evaluated by western blotting, in H460 cells treated with darbufelone 60 μM. **b** The protein level of caspase-3 in **a** was quantified. Histograms showed full-length and cleaved caspase-3 levels normalized to the β-actin, Data are presented as mean ± SEM of three separate experiments (*$p < 0.05$ vs. control, **$p < 0.01$ vs. control). **c** Darbufelone induced activation of caspase-8, as shown by cleaved fragments of casoase-8. **d** A time course of caspase-9, evaluated by western blot, in H460 cells treated with darbufelone 60 μM. **e** Western blotting analysis of bcl-2 and Bax expression in H460 cells harvested at different time points, in H460 cells treated with darbufelone 60 μM

tumor weight (data not shown). At necropsy, the tumor weight in mice treated with darbufelone (80 mg/kg/day) was reduced by 30.2% in comparison with control group (Fig. 5b).

To assess the anti-proliferation effect of darbufelone in vivo, we did Ki-67 staining on tumor sections, a well-accepted endogenous cell proliferation marker (Fig. 5c). Our data showed that darbufelone treatment significantly decreased positive Ki-67 staining by 33.5% in comparison with control group (Fig. 5d). Increased cleaved caspase-3 staining (2.1-fold), which indicates the occurrence of apoptosis, was also evident after darbufelone treatment (Fig. 5d). These results indicated that darbufelone treatment inhibits Lewis lung tumor growth through growth inhibition and apoptosis.

Discussion

Recently, a new class of anti-inflammatory drugs named dual COX/LOX inhibitors, interfering with both the production of prostaglandins and the biosynthesis of leukotrienes (LTs), has emerged as an alternative to avoid side effects related to COX inhibition. Although some of them have been implicated to have anti-cancer effects, no data are available concerning the potential use of dual COX/5-LOX inhibitors in lung cancer treatment up to date. In this regard, we applied darbufelone, which was well tolerated [14, 15], to observe its anticancer effect on lung cancers.

In the present study, we show for the first time that the dual COX/5-LOX inhibitor darbufelone possesses an anti-proliferation effect on human NSCLC cancer cell lines in vitro and Lewis lung cancer mice model in vivo. We demonstrated that this drug strongly decreased H460 viability in a time- and dose-dependent manner. The decrease of cell viability was associated with cell cycle arrest and apoptosis.

The findings are intriguing as different concentrations of darbufelone exhibit different mechanism of cell growth inhibition. When exposure to low concentration of darbufelone (20 μM), a G0/G1 cell cycle arrest was induced through up-regulation of p27, which is an important cancer suppressor gene, while the mRNA level of p53 and p21 did not change significantly. Up-regulation of p27 was associated with cell growth inhibition and G0/G1 phase arrest in human NSCLC cell lines [16]. And it is reported that p27 was up-regulated in response to the COX-2 inhibitor NS398 [17]. Therefore, it is reasonable to envision that COX-2 inhibition induced by darbufelone treatment increased the expression of p27 which afterwards resulted in cell growth inhibition.

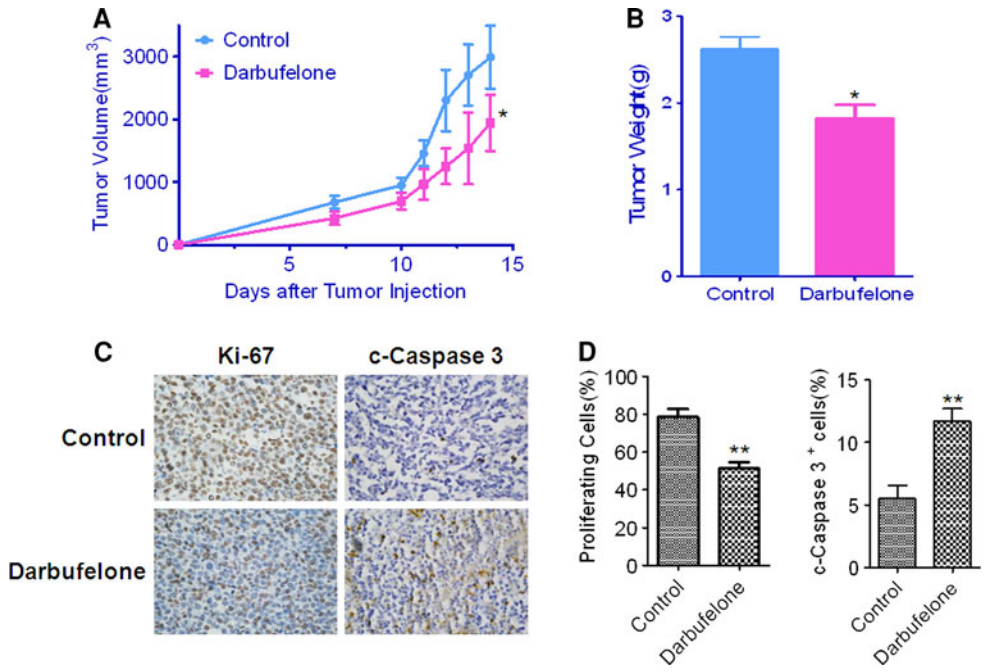

Fig. 5 Darbufelone inhibits the tumor growth in vivo. **a** Inhibitory effects of darbufelone on tumor volume in LLC-bearing mice over time. Tumor volumes were measured every other day. Data are presented as mean ± SEM, $n = 6$ mice per group (*$p < 0.05$ vs. control). **b** Effect of darbufelone on tumor weight at the termination of experiment on day 14. Data are presented as mean ± SEM, $n = 6$ per group. The statistically significant differences between control and sample groups were calculated by the Student's t test (*$p < 0.05$ vs. control). **c** Representative photomicrographs of proliferation detected by Ki-67 and tumor cell apoptosis detected by cleaved-caspase-3(c-Caspase-3). The sections were detected as DAB substrate staining (*brown*) and counterstained with Mayer's hematoxylin solution. **d** Data are presented as mean ± SEM, $n = 6$. Ki-67+ or c-caspase-3+ tumor cells were quantified in six random fields (400×). The statistically significant differences between control and sample groups were calculated by the Student's t test (*$p < 0.05$ vs. control, **$p < 0.01$ vs. control)

When exposed to high dose of darbufelone, H460 cells displayed the typical hallmarks of apoptosis, such as membrane bleb formation, irregularly fragmented pycnotic nuclei and caspase-3 activation. Investigations of apoptosis pathway revealed caspase-8 cleavage but not caspase-9, Bcl2, and Bax involved, suggesting that darbufelone-induced apoptosis is related to the extrinsic pathway. However, further experiment is necessary to clarify the detailed mechanism of apoptotic effect of darbufelone.

At last we used a mice model to verify the anti-tumor effect of darbufelone in vivo. Consistent with the anti-cancer effect in vitro, darbufelone treatment (80 mg/kg/day) significantly inhibited the Lewis lung carcinoma growth by 30%. As a new type of NSAIDs, darbufelone was proved to be a stronger potent analgesic compared to indomethacin, SC-51825 and NS-398. This relatively high dosage of darbufelone is believed to not only inhibit the growth of cancer but also alleviate the pain in cancer patients effectively; raising the possibility that darbufelone can be used as an adjunct with other anti-cancer agents in cancer chemotherapy.

NSCLC now accounts for approximately 75–85% of lung cancer cases and more than 60–65% of patients are diagnosed as having locally advanced or metastatic tumors with dismal prognosis [18]. Unfortunately, a considerable proportion of patients are not eligible for intensive chemotherapy because of age, performance status, or moribund conditions. The present findings may have a potential clinical meaning because administration of this kind of highly selective enzyme inhibitor alone or as an adjunct with other target-specific agents such as gefitinib (IRESSA®) may be feasible and provide more possibilities for individualized therapy without serious side effects in the future.

As we all know, COX-2 over-expression occurs not only in the tumor cells but also in the tumor vasculature [19], and inhibitors of COX-2 have anti-angiogenic activity [20]. Treatment with a selective COX-2 inhibitor celecoxib suppresses angiogenesis in mice model of lung cancer [21]. Meanwhile, inhibition of 5-LOX reduces production of leukotriene B4 (LTB4), which stimulates the growth of a wide range of human carcinomas. In addition, inhibition of 5-LOX was demonstrated to potently reduce production of VEGF. All of these findings indicate that a COX-2/5-LOX dual inhibitor may present a potential anti-angiogenic effect in chemotherapy [22]. Therefore, it will be interesting to investigate whether the effects of darbufelone on host cells, such as the inhibition of angiogenesis, can further enhance its anticancer effects in combination with other anticancer agents.

In summary, our study shows for the first time that darbufelone is able to induce cell cycle arrest, triggers apoptosis in lung cancer cells, and significantly inhibits lung tumor growth in mice. As a new member of NSAIDs, the dual COX/LOX-5 inhibitor darbufelone may represent a novel and promising approach to lung cancer chemotherapy.

Acknowledgments We appreciate the time and effort of Dr. Hongbin. Ji and Dr. Yan Ren in reviewing these manuscripts and we thank Li Li for technical support in IHC.

References

1. Jemal A, Siegel R, Ward E, Hao Y, Xu J, Murray T, Thun MJ (2008) Cancer statistics, 2008. CA Cancer J Clin 58:71–96
2. Nishizawa Y, Yamasaki M, Katayama H, Amakata Y, Fushiki S (2007) Establishment of a progesterone-sensitive cell line from human lung cancer. Oncol Rep 18:685–690
3. Levine L (1981) Arachidonic acid transformation and tumor production. Adv Cancer Res 35:49–79
4. McGiff JC (1987) Arachidonic acid metabolism. Prev Med 16:503–509
5. Achiwa H, Yatabe Y, Hida T, Kuroishi T, Kozaki K, Nakamura S, Ogawa M, Sugiura T, Mitsudomi T, Takahashi T (1999) Prognostic significance of elevated cyclooxygenase 2 expression in primary, resected lung adenocarcinomas. Clin Cancer Res 5:1001–1005
6. Hida T, Yatabe Y, Achiwa H, Muramatsu H, Kozaki K, Nakamura S, Ogawa M, Mitsudomi T, Sugiura T, Takahashi T (1998) Increased expression of cyclooxygenase 2 occurs frequently in human lung cancers, specifically in adenocarcinomas. Cancer Res 58:3761–3764
7. Wolff H, Saukkonen K, Anttila S, Karjalainen A, Vainio H, Ristimaki A (1998) Expression of cyclooxygenase-2 in human lung carcinoma. Cancer Res 58:4997–5001
8. Abou-Issa H, Alshafie G (2004) Celecoxib: a novel treatment for lung cancer. Expert Rev Anticancer Ther 4:725–734
9. Rioux N, Castonguay A (1998) Inhibitors of lipoxygenase: a new class of cancer chemopreventive agents. Carcinogenesis 19:1393–1400
10. Martin L, Rabasseda J, Castañer J (1999) Darbufelone mesilate—PD-136095-0073—CI-1004—antiarthritic—5-lipoxygenase inhibitor-COX-2 inhibitor. Drugs Future 24:853–857
11. Bannwarth B (2004) Is licofelone, a dual inhibitor of cyclo-oxygenase and 5-lipoxygenase, a promising alternative in anti-inflammatory therapy? Fundam Clin Pharmacol 18:125–130
12. Xu XL, Chen XJ, Ji H, Li P, Bian YY, Yang D, Xu JD, Bian ZP, Zhang JN (2008) Astragaloside IV improved intracellular calcium handling in hypoxia-reoxygenated cardiomyocytes via the sarcoplasmic reticulum Ca-ATPase. Pharmacology 81:325–332
13. O'Connor PM, Jackman J, Bae I, Myers TG, Fan S, Mutoh M, Scudiero DA, Monks A, Sausville EA, Weinstein JN, Friend S, Fornace AJ Jr, Kohn KW (1997) Characterization of the p53 tumor suppressor pathway in cell lines of the National Cancer Institute anticancer drug screen and correlations with the growth-inhibitory potency of 123 anticancer agents. Cancer Res 57:4285–4300
14. Britton MC (2000) American College of Rheumatology—63rd Annual Meeting. 13–17 November 1999, Boston, MA, USA. IDrugs 3:265–267
15. Rothschild B (2000) American College of Rheumatology—63rd annual meeting. 13–17 November 1999, Boston, MA, USA. IDrugs 3:158–163
16. Ling YH, Li T, Yuan Z, Haigentz M Jr, Weber TK, Perez-Soler R (2007) Erlotinib, an effective epidermal growth factor receptor tyrosine kinase inhibitor, induces p27KIP1 up-regulation and nuclear translocation in association with cell growth inhibition and G1/S phase arrest in human non-small-cell lung cancer cell lines. Mol Pharmacol 72:248–258
17. Hung WC, Chang HC, Pan MR, Lee TH, Chuang LY (2000) Induction of p27(KIP1) as a mechanism underlying NS398-induced growth inhibition in human lung cancer cells. Mol Pharmacol 58:1398–1403
18. Lee JM, Yanagawa J, Peebles KA, Sharma S, Mao JT, Dubinett SM (2008) Inflammation in lung carcinogenesis: new targets for lung cancer chemoprevention and treatment. Crit Rev Oncol Hematol 66:208–217
19. Masferrer JL, Leahy KM, Koki AT, Zweifel BS, Settle SL, Woerner BM, Edwards DA, Flickinger AG, Moore RJ, Seibert K (2000) Antiangiogenic and antitumor activities of cyclooxygenase-2 inhibitors. Cancer Res 60:1306–1311
20. Skopinska-Rozewska E, Piazza GA, Sommer E, Pamukcu R, Barcz E, Filewska M, Kupis W, Caban R, Rudzinski P, Bogdan J, Mlekodaj S, Sikorska E (1998) Inhibition of angiogenesis by sulindac and its sulfone metabolite (FGN-1): a potential mechanism for their antineoplastic properties. Int J Tissue React 20:85–89
21. Klenke FM, Gebhard MM, Ewerbeck V, Abdollahi A, Huber PE, Sckell A (2006) The selective Cox-2 inhibitor Celecoxib suppresses angiogenesis and growth of secondary bone tumors: an intravital microscopy study in mice. BMC Cancer 6:9
22. Edelman MJ, Watson D, Wang X, Morrison C, Kratzke RA, Jewell S, Hodgson L, Mauer AM, Gajra A, Masters GA, Bedor M, Vokes EE, Green MJ (2008) Eicosanoid modulation in advanced lung cancer: cyclooxygenase-2 expression is a positive predictive factor for celecoxib + chemotherapy—cancer and leukemia group B trial 30203. J Clin Oncol 26:848–855